Sizing of Lecithin-Bile Salt Mixed Micelles by Size-Exclusion High-Performance Liquid Chromatography†

J. Wylie Nichols* and Justyna Ozarowski

Department of Physiology, Emory University School of Medicine, Atlanta, Georgia 30322

Received November 20, 1989; Revised Manuscript Received January 24, 1990

ABSTRACT: Size-exclusion high-performance liquid chromatography with a TSK 5000 PW column was shown to be a fast and relatively inexpensive method for the size determination of lecithin-bile salt mixed micelles. Perturbation of the equilibrium between aqueous soluble and micellar bile salts during elution was avoided by preequilibration of the column with buffer containing the aqueous soluble concentration of the bile salt. Elution volumes were converted to size dimensions from a calibration curve produced from the elution volumes of proteins and small unilamellar vesicles of known size. Micelle sizes determined for several different lecithin-bile salt mixtures were consistent with those obtained by other techniques. The well-known hyperbolic increase in mixed micelle size as the lecithin to bile salt ratio approaches the micellar-vesicle phase limit was reproduced with this chromatographic technique. On the basis of these data and the recent observation by small-angle neutron scattering that lecithin-bile salt micelles increase in size by the elongation of constant-diameter rods [Hjelm et al. (1988) *J. Appl. Crystallogr. 21*, 858-863], a new model for the mixed micelle structure is proposed. According to this model, separation of the lecithin head groups by bile salts inserted along the rod surface produces a radial orientation of lecithin molecules along the length of the rod. Each end of the rod is sealed off by a lecithin-bile salt configuration that is richer in bile salts than the rod portion of the micelle. A simple mathematical description of this model predicts the observed changes in micellar size as a function of the lecithin-bile salt ratio with parameters that are consistent with lecithin and bile salt molecular dimensions.

Long-chain phospholipids and bile salts spontaneously aggregate to form mixed micelles or vesicles, depending on the ratio of phospholipid to bile salt in the lipid aggregate—bile salt rich aggregates form micelles while phospholipid-rich aggregates form vesicles. Because of the higher aqueous solubility of bile salts (1-20 mM; Small, 1971; Roda et al., 1983) relative to long-chain phospholipids (in the nanomolar range; Smith & Tanford, 1972), large changes in the phospholipid to bile salt ratio within the aggregate occur when the lipid mixture is either concentrated or diluted. Thus, the structural arrangement of these lipid aggregates changes during the concentration of phospholipid-bile salt mixtures that occurs in the gallbladder and their dilution upon gallbladder emptying into the duodenum. It is therefore important to determine the changes in structural arrangement and size that occur as a result of concentration and dilution of these lipid mixtures. Once this has been accomplished, we will be better able to understand the role of phospholipids and bile salts in the solubilization of cholesterol, bile pigments, and other lipid excretory products in the bile as well as to understand the role of these lipid aggregates during lipid digestion and absorption.

With this in mind, we developed a simple, fast, and relatively inexpensive technique for determining the sizes of populations of phospholipid-bile salt mixed micelles based on their elution volume through a size-exclusion high-performance liquid chromatography (HPLC)[1] column (TSK 5000 PW). Although other techniques such as quasi-elastic light scattering (QELS; Mazer et al., 1980; Schurtenberger et al., 1985), nuclear magnetic resonance (NMR; Schurtenberger & Lindman, 1985), X-ray small-angle scattering (XSAS; Müller, 1981, 1984), and small-angle neutron scattering (SANS; Hjelm et al., 1988, 1990) are available for determining the size of phospholipid-bile salt mixed micelles, they are time-consuming and require expensive equipment that is not widely available. X-ray and neutron scattering have the potential to give more detailed information regarding aggregate shape and dimensions, while QELS, NMR, and size-exclusion HPLC infer the size from a related measured parameter. The QELS and NMR techniques use the Stokes-Einstein equation to infer the micelle or aggregate size from the measured diffusion coefficient, whereas the size-exclusion HPLC technique uses the elution volume of the aggregate as it passes through the size-exclusion column to infer the size. The size-exclusion HPLC technique requires only standard HPLC equipment and should be readily adapted to the specific needs of researchers who study the properties of phopholipid-bile salt aggregates.

We have combined the size information obtained from our studies using size-exclusion HPLC with lecithin-bile salt micelle size and shape information obtained from SANS (Hjelm et al., 1988, 1990) to propose a new model for the structural arrangement of these mixed micelles. As opposed to the widely accepted mixed disk model (Mazer et al., 1980) in which lecithin molecules are assumed to aggregate with bile salt dimers into a disk-shaped bilayer with its periphery sur-

† This study was supported by U.S. Public Health Service Grants GM32342 and DK40641.

* To whom correspondence should be addressed.

[1] Abbreviations: HPLC, high-performance liquid chromatography; XSAS, X-ray small-angle scattering; QELS, quasi-elastic light scattering; SANS, small angle neutron scattering; NMR, nuclear magnetic resonance; POPC, 1-palmitoyl-2-oleoylphosphatidylcholine; DOPC, dioleoylphosphatidylcholine; TBS, Tris-buffered saline [150 mM NaCl in 10 mM tris(hydroxymethyl)aminomethane, pH 8.5]; HBS, HEPES-buffered saline [150 mM NaCl in 10 mM 4-(2-hydroxyethyl)-1-piperazineethanesulfonic acid, pH 7.4]; CMC, critical micelle concentration.

0006-2960/90/0429-4600$02.50/0

rounded by additional bile salt molecules, we propose that phospholipids and bile salts are arranged radially in the shape of rods with their ends protected by bile salt rich caps.

Experimental Procedures

Materials and Routine Procedures. The phospholipids 1-palmitoyl-2-oleoylphosphatidylcholine (POPC) and dioleoylphosphatidylcholine (DOPC) (Avanti Polar Lipids, Inc.) were found to be greater than 99% pure by silica gel thin-layer chromatography. The sodium salts of deoxycholate, cholate, taurodeoxycholate, taurocholate, glycodeoxycholate, glycocholate, and chenodeoxycholate were purchased from Sigma Chemical Co. Bile salts were tested by thin-layer chromatography, found to be greater than 98% pure, and used without further purification. Liquid scintillation counting following thin-layer chromatography of radiolabeled 1,2-dipalmitoylphosphatidyl[*N-methyl*-^{3}H]choline (73 Ci/mmol, Amersham) and deoxycholic acid (carbonyl-^{14}C) (50 mCi/mmol, ICN Biochemicals) indicated greater than 95% purity of the former and 98% purity of the latter. NaCl (J. T. Baker), HEPES (United States Biochemical), and Tris (Sigma) were ACS or reagent-grade. Water was deionized and purified with a Milli-Q water system (Millipore). Phospholipid concentrations were determined by a lipid phosphorus assay (Ames & Dubin, 1960). Globular proteins used for column standards were purchased from Sigma Chemical Co. Vesicles used for column calibration were prepared by bath sonication, and a Nicomp 370 submicron particle sizer (Pacific Scientific) was used to determine their size as described by Menger et al. (1989).

High-Performance Liquid Chromatography. High-performance liquid chromatography was performed with a Rainin Rabbit-HP pump with 5-mL pump heads. Separations were made with a Spherogel TSK 5000 PW column (Beckman) preceded by a 0.5-μm in-line filter. Micelles and proteins were detected by optical density changes at 280 nm with a Spectromonitor D variable-wavelength detector (LDC/Milton Roy), and the signal was recorded with a Shimadzu Chromotopac C-R3A. Peak elution volumes were determined by the recorder from the OD_{280} traces. Fractions were collected with a Gibson Model 201 fraction collector. Aliquots of 50–100 μL were injected and run at a maximum flow rate of 1 mL/min. At this flow rate, the inlet pressure never exceeded 12 kg/cm^2 ($\sim$170 psi). The total volume of the column was determined from the elution volume of sodium azide (V_t = 11.13 mL). The column-excluded volume was determined from the elution volume of large multilamellar liposomes (V_o = 4.92 mL). Elution volumes of samples are presented as K_d, where $K_d = (V_e - V_t)/(V_t - V_o)$; V_e is the volume eluted at the sample peak.

Micelle Preparation and Column Sizing. Lecithin–bile salt mixed micelles were prepared by mixing the desired amounts of lecithin and bile salt dissolved in chloroform/methanol (1:1). The solvents were removed with a stream of nitrogen followed by a minimum of 4 h of desiccation under vacuum. The lipids were suspended in 1–3 mL of buffer, vortex-mixed until clear, placed in Spectropor 3 dialysis bags (molecular weight cutoff 3500), and dialyzed against the desired concentration of bile salt in 0.5–1.0 L of buffer for a minimum of 18 h at room temperature. Following dialysis, the TSK 5000 PW column was equilibrated with 150 mL of the dialysis buffer. The mixed micelle solutions were removed from the dialysis bags, and 50–100-μL aliquots were injected onto the column.

Experiments with POPC–deoxycholate mixed micelles in TBS were quantified by incorporating trace amounts of [^{3}H]dipalmitoylphosphatidylcholine and [^{14}C]deoxycholate. In these experiments, the micelle solutions and the dialysis buffer were prepared from the same radiolabeled stock deoxycholate so that the specific activity of deoxycholate was the same for both. Equilibration of the column with [^{14}C]-deoxycholate was assumed to be complete when no significant difference was found between the ^{14}C counts in the dialysis buffer before and after elution from the column. In all cases, elution with 150 mL was sufficient to obtain complete equilibration, and this volume was assumed to result in column equilibration when other bile salts were used. Half-milliliter aliquots of the column eluant were collected, and the amount of deoxycholate and POPC in each was determined by dual liquid scintillation counting of ^{3}H and ^{14}C. Background counts in the first five void volume fractions were averaged and subtracted from the counts in subsequent fractions to obtain the amount of micellar POPC and deoxycholate. All experiments and dialysis were performed at room temperature ($\sim$22 °C).

Results

Elution Volume Varies with the Ratio of POPC to Deoxycholate. As a test of the accuracy and usefulness of size-exclusion HPLC for the size determination of lecithin–bile salt micelles, we measured the expected increase in the size of mixed micelles as the ratio of lecithin to bile salt was increased (Mazer et al., 1980; Schurtenberger et al., 1985; Müller, 1981, 1984; Hjelm et al., 1988, 1990). The ratio of POPC to deoxycholate in the micelles was varied in a controlled and predictable fashion by dialyzing the POPC and deoxycholate micelles (total concentration 10 mM deoxycholate and 10 mM POPC) against excess TBS buffer containing deoxycholate at different concentrations below the critical micelle concentration (CMC). After equilibration, the concentration of the aqueous soluble deoxycholate in equilibrium with the POPC–deoxycholate micelles (defined as the intermicellar concentration or IMC) is the same as the starting concentration of deoxycholate in the dialysis buffer. Depending on the relative magnitude of the IMC for the POPC–deoxycholate micelles and the concentration of deoxycholate in the dialysis buffer, the micelles will either gain or lose deoxycholate to achieve equilibrium. In this way, the phospholipid to bile salt ratio in the micelles can be systematically altered. To avoid perturbation of the equilibrium between aqueous soluble and micellar bile salts during column elution, the column was preequilibrated with the buffer used for dialysis.

The elution profiles of POPC–deoxycholate mixed micelles dialyzed against different concentrations of deoxycholate are presented in Figure 1. These data illustrate that as the concentration of deoxycholate in the dialysis buffer is reduced, the ratio of POPC to deoxycholate in the micellar peak increases, and the elution volume decreases, indicating an increase in size. In the experiments presented in Figure 1, no detectable POPC is retained on the column; the total amount of POPC eluted in each experiment is essentially constant and equal to the amount injected (0.5 μmol). The peak elution volumes of the micelles were not dependent on the flow rate (1 mL/min or less) or the column pressure (<170 psi) (data not shown).

Mixed micellar solutions dialyzed against deoxycholate concentrations of 0.7 mM or less were eluted at or close to the excluded volume of the column, and a significant fraction of the POPC was retained on the prefilter or the column. In this range, a small decrease in the concentration of deoxycholate in the dialysis buffer resulted in a large increase in the size of the mixed micelles.

Column Calibration. Globular proteins of known hydrodynamic radius (14.5–69.5 Å) and phospholipid vesicles (142

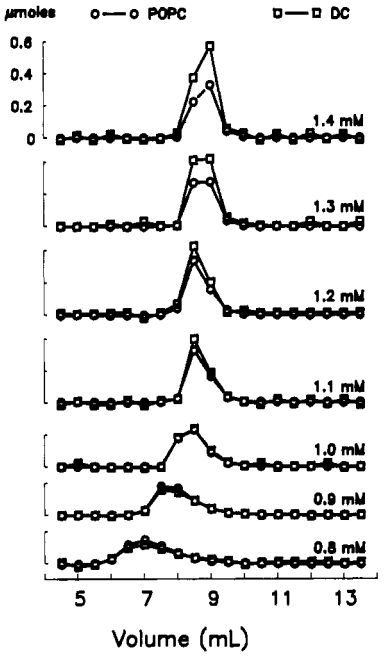

FIGURE 1: Elution profiles of POPC–deoxycholate micelles equilibrated against different concentrations of deoxycholate. Mixed micelles containing equimolar mixtures of POPC and deoxycholate (20 mM total) containing trace amounts of ^{3}H-labeled dipalmitoylphosphatidylcholine and [^{14}C]deoxycholate were prepared with TBS and dialyzed against various concentrations of [^{14}C]deoxycholate in TBS (concentrations are printed to the right of each elution profile). The specific activity of the [^{14}C]deoxycholate was identical in the micelle solutions and the dialysis buffer. Fifty microliters of the dialyzed micelle mixture containing 0.5 μmol of POPC was injected into the column, and 0.5-mL samples were taken and counted by dual-label liquid scintillation counting. [^{14}C]Deoxycholate and [^{3}H]dipalmitoylphosphatidylcholine in the column void volume fractions were averaged and subtracted from their respective counts in all the fractions, and the amounts of each above background were plotted [(○) POPC; (□) deoxycholate]. The ratio of POPC to deoxycholate was calculated from their sums under each peak. Elution volumes were determined from peaks of absorbance traces at 280 nm.

Å) were used to calibrate the TSK 5000 PW column according to the empirical equation of Ackers (1967) (Nozaki et al., 1976):

$$R = a_0 + b_0 \, \mathrm{erf}^{-1}(1 - K_d) \qquad (1a)$$

where K_d is the distribution coefficient (see definition under Experimental Procedures) and a_0 and b_0 are constants that reflect the pore size distribution of the gel. The function $\mathrm{erf}^{-1} x$ is the inverse of the error function of the Gaussian distribution where $\mathrm{erf}\, x = 1 - (2/\pi^{1/2}) \exp(-x^2)\, dx$. Values of $\mathrm{erf}^{-1}(1 - K_d)$ were obtained from a table of error functions (NBS Applied Mathematics Series 41). Equation 1a has been shown to yield a linear plot of the molecular radius of globular proteins for a wide range of size-exclusion columns (Ackers, 1967; Nozacki et al., 1976). Figure 2 illustrates this linear relationship for the TSK 5000 PW column for the protein and vesicle standards.

Micelle Size Is Dependent on the Ratio of POPC to Deoxycholate. Data for the elution volumes of mixed micelles of known POPC to deoxycholate ratio, obtained as illustrated in Figure 1, were converted to hydrodynamic radii by using the calibration plot in Figure 2 and plotted as a function of the POPC to deoxycholate ratio (Figure 3). Each symbol type refers to a different concentration of deoxycholate in the dialysis buffer. As expected from the previous work of others (Mazer et al., 1980; Schurtenberger et al., 1985; Müller, 1981, 1984; Hjelm et al., 1988, 1990), the hydrodynamic radius increases as a hyperbolic function of the ratio of lecithin to

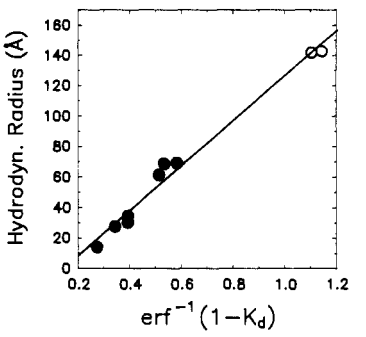

FIGURE 2: Calibration curve for the TSK 5000 PW column. Globular proteins (●) and phospholipid vesicles (○) were used to calibrate the column. Protein standards and radii were as follows: bovine serum albumin, 30.6 Å; lactate dehydrogenase, 34.7 Å; lactalbumin, 14.5 Å (radii determined by X-ray diffraction; Kumosinski & Pesson, 1985); ovalbumin, 27.9 Å; apoferritin, 61.6 Å; thyroglobulin, 69.5 Å (radii determined from hydrodynamic relationship of molecular weight to molecular volume; Himmel & Squire, 1981); β-galactosidase, 69 Å (radius determined by sedimentation equilibrium and hydrodynamic measurements; Nozaki et al., 1976). Vesicles were prepared from distearoylphosphatidylcholine/distearoylphosphatidic acid (95:5 mol %), 143 Å, and dipalmitoylphosphatidylcholine/distearoylphosphatidic acid (95:5 mol %), 142 Å [radii determined by QELS as described by Menger et al. (1989)]. See Experimental Procedures for explanation of the inverse error function of $1 - K_D$. The calibration line is radius = 148 [$\mathrm{erf}^{-1}(1 - K_D)$] − 20.2.

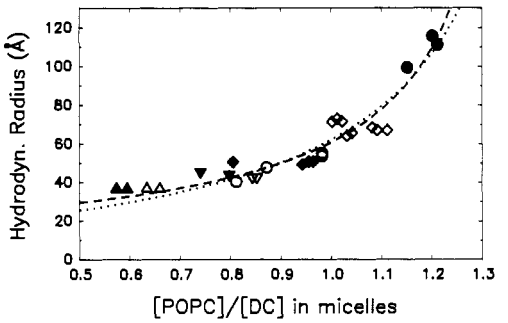

FIGURE 3: Hydrodynamic radius versus the micellar ratio of POPC to deoxycholate. Micelles containing different ratios of POPC and deoxycholate were prepared by dialysis against varying concentrations of deoxycholate. Ratios of POPC to deoxycholate in the micellar peaks were measured as described in the legend to Figure 1, and the hydrodynamic radii were determined from the peak elution volumes by using the calibration line in Figure 2. Symbols refer to measurements made with the same deoxycholate concentration in the dialysis buffer: (●) 0.8 mM; (◇) 0.9 mM; (◆) 1.0 mM; (▽) 1.1 mM; (▼) 1.2 mM; (△) 1.3 mM; (▲) 1.4 mM. Data from Table I are presented as (○). The dotted line is the best fit of the data to the mixed-disk model, and the dashed line is the best fit to the capped-rod model.

deoxycholate in the micelles. The dotted line is the best fit of these data to the mixed-disk model (Mazer et al., 1980) and the dashed line the best fit of an alternative model based on micelle growth in the shape of rods which will be presented under Discussion.

Micelle Size Is Dependent on Phospholipid Concentration. Table I presents the results of an experiment where different starting amounts of POPC and deoxycholate in a 1:1 molar ratio were dialyzed against the same concentration of deoxycholate (1 mM). The results indicate that as the mixed micellar concentration is increased, the ratio of POPC to deoxycholate and the micelle size both increase. Since the concentration of free deoxycholate in equilibrium with the mixed micelles is held constant by the excess in the dialysis buffer, one would expect that at equilibrium the distribution of free and micellar deoxycholate would be independent of the concentration of POPC. One possible explanation for this anomaly is that at higher micelle concentrations, micelle in-

Table I: Dependence of Micellar Size on Phospholipid Concentration[a]

[POPC] (mM)	[POPC]/[DC][b]	K_d[c]	$erf^{-1}(1 - K_d)$[d]	radius[e] (Å)
5	0.81	0.557 (0.001)	0.415 (0.001)	41.1 (±6.9)
10	0.87	0.518 (0.003)	0.457 (0.003)	47.2 (±6.9)
20	0.98	0.482 (0.003)	0.498 (0.003)	53.2 (±6.8)
30	0.98	0.465 (0.008)	0.516 (0.009)	56.0 (±6.8)

[a] Equimolar mixtures of POPC and deoxycholate were prepared with the designated concentrations of POPC in TBS buffer and dialyzed against 1.0 mM deoxycholate in TBS buffer. The TSK 5000 PW column was equilibrated with the dialysis buffer, and 50 μL of the micelle mixture was injected onto the column. [b] Phospholipid to deoxycholate ratio in the micelles was calculated from the radiolabeled counts as described under Experimental Procedures. [c] K_d is defined under Experimental Procedures. The numbers are the average of two column runs. The difference between the two values is presented in parentheses. [d] The use of the error function for column calibration is presented under Results (Column Calibration). [e] The radii were calculated by using the calibration line presented in Figure 2. The numbers in parentheses are the standard errors of the predicted values (Snedecor & Cochran, 1967).

teraction reduces the activity of the micelles. The lowered activity slows the rate of free deoxycholate association with the micelles without changing the rate of deoxycholate dissociation from the micelles, resulting in a reduction of the amount of micellar deoxycholate in equilibrium with the free deoxycholate.

When the data in Table I are plotted in Figure 3 (open circles), they fall in line with the previous data relating size to the ratio of POPC to deoxycholate and further support that this ratio dictates the micelle size regardless of the total lipid concentration. This result also argues against the possibility that the observed size increase at higher concentrations results from micelle interactions during column elution.

Dependence of Micelle Size on Structure of Bile Salts. Table II presents data where the Spherogel TSK 5000 PW column was used to determine the size of lecithin–bile salt micelles prepared from several different bile salts. The starting concentrations of DOPC and bile salt (10 and 20 mM, respectively) were the same for each case. The intermicellar bile salt concentration for each mixture was determined by a null-point light-scattering technique described previously (Shankland, 1970; Nichols, 1988), and the micellar mixtures were dialyzed against their respective IMCs. The columns were equilibrated with HBS containing the IMC of the respective bile salt and the elution volume and sizes of the mixed micelles determined. The ratio of DOPC to bile salt for each mixed micelle was estimated by subtracting the measured IMC from the total concentration of bile salt and dividing this difference into the DOPC concentration. All of the predicted ratios fall between 0.53 and 0.71 and the hydrodynamic radii between 35.0 and 45.9 Å.

Discussion

We have demonstrated the feasibility of using size-exclusion HPLC (TSK 5000 PW column) for determining the sizes of mixed lecithin–bile salt micelles with hydrodynamic radii in the range of 10–150 Å. A TSK 6000PW size-exclusion HPLC column has been used previously to determine the sizes of phospholipid vesicles and virus particles in the range of 100–1000-Å radius (Ollivon et al., 1986). We have addressed the importance of equilibrating the column with the IMC of the appropriate bile salt and have found that by doing so we can measure the sizes of a wide range of bile salts with results that are consistent with several other techniques, e.g., quasi-elastic light scattering (QELS), X-ray small-angle scattering (XSAS), nuclear magnetic resonance (NMR), and small-angle neutron scattering (SANS).

Comparison of mixed micelle sizes measured by different techniques is complicated by the sensitivity of the micelle size to temperature, the ratio of the components, their concentration, ionic strength, and pH. Most experiments have been done under conditions similar to those used in this study, i.e., 150 mM NaCl, pH ~7, and temperature ~20 °C. It is more difficult to adjust for the wide range of concentrations and molar ratios used in various studies. However, since the ratio of lecithin to bile salt in the micelle is the major determinant of size for given temperatures, ionic strength, and pH, a reasonable comparison of the different techniques can be made if this ratio is provided or can be inferred from the data. Mazer et al. (1980) determined the hydrodynamic radius of lecithin–taurocholate micelles to be ~24 Å for a calculated micellar lecithin to taurocholate ratio of 0.6. This is somewhat smaller than the equivalent measurement in Table II; however, in another QELS study, Schurtenberger et al. (1985) measured hydrodynamic radii of 40 and 80 Å for micellar lecithin–glycocholate ratios of 0.6 and 1.13. The value at 0.6 is very close to the 41.8-Å radius measured for a micellar ratio of 0.67 by size-exclusion HPLC. A smaller hydrodynamic radius of 33 Å for a similar micellar ratio of lecithin to taurocholate of 0.65—calculated by assuming an IMC for the mixture of 4.8 mM (Table II)—was measured by NMR (Schurtenberger & Lindman, 1985). XSAS (Müller, 1984) gives a value of 45 Å for a micellar ratio (lecithin to taurodeoxycholate) of 0.67. The SANS data (Hjelm et al., 1988) are not in a ratio range that allows direct comparison with the lecithin–glycocholate micelles in Table II. However, the micellar ratio of lecithin to glycocholate of 1.0, which produced a prolate ellipsoid with semiaxes of 27.5 and 133 Å or a calculated hy-

Table II: Size Comparison of Micelles Prepared from Different Bile Salts[a]

bile salt	IMC (mM)	[DOPC]/[BS][b]	K_d[c]	$erf^{-1}(1 - K_d)$[d]	radius[e] (Å)
taurodeoxycholate	1.0	0.53	0.597 ± 0.001 (4)	0.374 ± 0.001	35.0 ± 7.0
glycodeoxycholate	1.0	0.53	0.586 ± 0.006 (4)	0.384 ± 0.006	36.5 ± 7.0
deoxycholate	1.6	0.54	0.528 ± 0.005 (5)	0.446 ± 0.005	45.5 ± 6.9
chenodeoxycholate	1.9	0.55	0.526 ± 0.008 (4)	0.448 ± 0.008	45.9 ± 6.9
taurocholate	4.8	0.66	0.537 ± 0.005 (4)	0.436 ± 0.005	44.2 ± 6.9
glycocholate	5.0	0.67	0.552 ± 0.001 (4)	0.421 ± 0.001	42.0 ± 6.9
cholate	5.9	0.71	0.536 ± 0.003 (4)	0.437 ± 0.003	44.3 ± 6.9

[a] Micelles containing 10 mM DOPC and 20 mM of the designated bile salt were prepared in HBS buffer, and the IMC was measured by the null-point light-scattering technique described under Experimental Procedures. The TSK 5000 PW column was equilibrated with HBS containing the IMC of the corresponding bile salt. Fifty microliters of micelles was injected onto the column and the size determined from the elution volume by using the calibration curve in Figure 2 as described under Experimental Procedures. [b] The ratio of DOPC to bile salt was estimated by dividing the total concentration of DOPC by the total concentration of bile salt minus the IMC. [c] K_d is defined under Experimental Procedures. The numbers are the average of several column runs ± the standard deviation. The number of column runs is in parentheses. [d] The use of the error function for column calibration is presented under Results (Column Calibration). [e] The radii were calculated by using the calibration line presented in Figure 2. Standard errors of the predicted values are given (Snedecor & Cochran, 1967).

drodynamic radius of 47.6 Å (eq 4), compares favorably with the hydrodynamic radius of 60 Å measured for a micellar lecithin to deoxycholate ratio of 1.0 (Figure 3). These data illustrate that the size-exclusion HPLC technique gives hydrodynamic radii that are well within the statistical error of observations made by other techniques. The advantages of size-exclusion HPLC are that it is fast and the equipment is less expensive than any of the scattering techniques. By combining the null-point light-scattering technique for measuring the IMC (Shankland, 1970; Nichols, 1988) with size-exclusion HPLC, the size distribution of particles from natural bile as well as artificial bile can be determined.

One disadvantage of this technique is that the effect of particle shape on the elution volume has not been determined. One has to assume that the theoretical relationships derived to relate the hydrodynamic volumes of spheres, prolate, and oblate ellipsoids, disks, and rods in solution also predict their elution through the pores of the column resin. The similarity between the hydrodynamic radii inferred from the elution volume obtained from size-exclusion HPLC with those inferred from the diffusion constants obtained from QELS and NMR suggests that the hydrodynamic radius provides a reasonable prediction of the elution volume within the size range used in this study. Deviations from these relationships are likely to occur for particles in which one axis is much larger than the other (e.g., long thin rods or large flat disks).

The currently accepted model for the shape of lecithin–bile salt micelles is the mixed-disk model proposed by Mazer et al. (1980). According to this model, phospholipid molecules are arranged in a circular bilayer forming a disk with bile salt dimers intercalated within the bilayer as well as surrounding its periphery. The most compelling argument in favor of the mixed-disk model is the intuitive simplicity with which the model explains the observed hyperbolic increase in micelle size as the ratio of lecithin to bile salt in the micelle is increased, and the internal consistency between the molecular sizes of the lecithin and bile salt components predicted from the model with those measured independently by other means. This relationship was demonstrated initially by using quasi-elastic light scattering to measure the size of egg lecithin–taurocholate micelles (Mazer et al., 1980). We have demonstrated a similar relationship for lecithin–deoxycholate micelles in Figure 3.

The physical data in support of the disk shape for these micelles are not conclusive, however. Mazer et al. (1980) argued that circular particles seen in negative-stain transmission electron micrographs were flat disks, but the smallest disks observed were 80–100 Å in radius for particles that were measured to be 35-Å radius by QELS. Assuming the QELS measurements are correct, the reliability of negative-stain transmission electron microscopy for determing the size and shape of micelles becomes questionable. In the same paper, the disklike shape of the mixed micelles was also deduced from a quantitative analysis of the dependence of the time-averaged scattered light intensity on the hydrodynamic radius. The experimental data fall between those predicted for disks and those for rods. After correction of the experimental data for the effects of polydispersity, the data favored the disk over the rod shape for the micelles, but the rod shape could not be conclusively ruled out. On the basis of XSAS data, Müller (1981) also concluded that 1:1 mole ratio mixtures of lecithin–glycocholate formed mixed micelles with a disk shape. However, owing to the low inherent contrast between the micelles and the water solvent, accurate measurements of low concentrations of micelles were not possible. Data obtained at high concentrations (10% w/v) were confounded by interparticle interference, and since the relative contributions of micelle size and interparticle interference to the distance distribution function could not be determined, the conclusion that the disk shape produces a theoretical real-space distance distribution function that most closely resembles that obtained experimentally for the lecithin–glycocholate micelles cannot be considered conclusive evidence that these mixed micelles are disk-shaped.

Recently, Hjelm et al. (1988, 1990) presented SANS data that are not consistent with the disk shape but instead indicate that lecithin–glycocholate micelles are rod-shaped and that growth of the micelles upon dilution occurs by elongation of the rod with a constant radius of 27 Å. The high signal to noise ratio obtained in these experiments allowed for accurate scattering measurements to be obtained as lecithin–glycocholate micelles were diluted from 50 to 1 mg/mL for mole ratios of 0.56 and 0.9. These data demonstrate that lecithin–glycocholate micelles are in the shape of prolate ellipsoids at high concentrations and upon dilution elongate along a single axis to form long rods with a constant radius. These data do not support micelle growth as an increase in the disk radius as predicted by the mixed-disk model. The rod shape has also been proposed from NMR studies for the hexagonal phase of lecithin–cholate mixtures (Lindblom et al., 1984). In addition a rod-shaped structure has been demonstrated for lecithin–cholate micelles (Walter et al., 1990) and lecithin–octyl glucoside micelles (Vinson et al., 1989) by cryotransmission electron microscopy.

Hjelm et al. (1990) argued that the lecithin–glycocholate rods were most likely formed by the stacking of basic disklike unit structures as suggested earlier by Shankland (1970). However, according to this model, one would predict that the decrease in micelle concentration upon dilution would decrease the probability of self-association into stacked disks, and therefore decrease the rod length. To account for the observed size increase, one would have to postulate that removal of the bile salts from the disks during dilution alters the micelle structure so as to increase the likelihood of disk self-association. It is not apparent why decreasing the amount of bile salt in the micelle would favor micelle association.

Given the current disagreement in the interpretation of the physical data pertaining to the shape of the lecithin–bile salt mixed micelle, we have developed an alternative model based on the rod-shaped morphology that is consistent with the radial dimension determined by SANS and which explains the elongation of the rods as the micellar ratio of lecithin to bile salt is increased. According to this model, lecithin and bile salt molecules aggregate to form a rod with the lecithin molecules oriented radially with their head groups facing outward toward the water. Bile salts insert between and separate the phospholipid head groups to provide sufficient curvature for the radial orientation (Figure 4). The hydrophobic surfaces at both ends of these rods are protected by bile salt rich caps. The radius of the rod is assumed to be constant along its length, and the phospholipid to bile salt ratio within the rod portion is assumed to remain constant at that ratio which produces the lowest free energy for the rod configuration. The phospholipid to bile salt ratio in each of the caps is predicted to be lower than in the rod and also remains constant at that ratio which provides the lowest free energy configuration necessary to protect the hydrophobic ends of the rod from the polar solvent. We designated this the "capped rod" model, and using these basic assumptions, we can derive a simple theoretical relationship that explains the dependence of the rod length on the lecithin to bile salt ratio in the entire

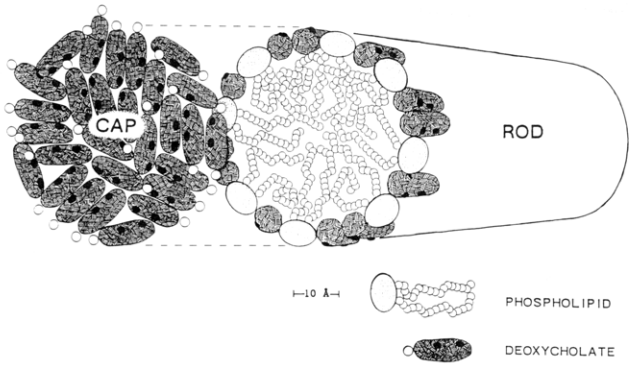

FIGURE 4: Capped-rod model for lecithin–deoxycholate mixed micelles. The proposed deoxycholate cap is pulled away to show the arrangement of lecithin and deoxycholate molecules in the rod portion of the micelle. The numbers of phospholipid and deoxycholate molecules in the cap and rod were derived from the parameters giving the best fit of the capped-rod model (eq 2) to the data in Figure 3. The best-fit parameter for α/β (the lecithin to deoxycholate ratio in the rod portion of the micelle) is 1.4. Since the molecular surface area of a bile salt lying along the rod surface is roughly equivalent to that of two lecithin molecules inserted radially, the number of lecithin and deoxycholate molecules projected onto the edge of the rod is 8 and 12, respectively. The best-fit parameter for a/b (the lecithin to deoxycholate ratio in the caps) is zero; thus, the cap is drawn to contain only deoxycholate molecules. However, the capped-rod model does not preclude the existence of phospholipids in the caps (see Discussion for details).

micelle (rod plus caps). Define α as the number of phospholipids per length and β as the number of bile salts per length of the rod portion of the micelle, and a as the number of phospholipid and b as the number of bile salts in each cap. Thus, the ratio of phospholipid to bile salt in the micelle is equal to

$$\frac{PC}{BS} = \frac{\alpha L + 2a}{\beta L + 2b} \quad (1)$$

where PC and BS are the number of lecithin and bile salt molecules in the micelle, respectively, and L is the length of the rod portion. Solving for L yields

$$L = \frac{2b(PC/BS - a/b)}{\beta(\alpha/\beta - PC/BS)} \quad (2)$$

for $a/b \leq PC/BS < \alpha/\beta$. The relationship predicts a hyperbolic increase in L as a function of PC/BS. As PC/BS approaches a/b (the ratio in the caps), L approaches zero, and as PC/BS approaches α/β (the ratio in the rod), L approaches infinity (i.e., the micellar phase limit).

The mixed-disk model predicts that the disk radius will increase as the micellar lecithin to bile salt ratio increases, according to the equation:

$$r = \frac{(2p/\sigma)(PC/BS)}{1 - \gamma^{-1}(PC/BS)} \quad (3)$$

where r is the disk radius, p is the number of bile salts per unit length of the disk's perimeter, σ is the number of lecithin molecules per unit area of the mixed bilayer, γ is the ratio of lecithin to bile salt molecules in the mixed bilayer, and PC and BS are the total numbers of lecithin and bile salt in the micelle.

The capped-rod model and the mixed-disk model were tested for their ability to predict the experimental data in Figure 3. The hydrodynamic radii obtained from the elution volumes of the size-exclusion column were converted to rod lengths (eq 4) assuming a constant rod radius of 27 Å and disk radii (eq 5) assuming a constant thickness of 60 Å according to the

$$R_h = (3/4)d\{[1 + (L/d)^2]^{1/2} + (d/L)\ \ln[L/d + [1 + (L/d)^2]^{1/2}] - L/d\}^{-1} \quad (4)$$

$$R_h = (3/2)r\{[1 + (t/2r)^2]^{1/2} + (2r/t)\ \ln[t/2r + [1 + (t/2r)^2]^{1/2}] - t/2r\}^{-1} \quad (5)$$

relationships presented by Mazer et al. (1980) where R_h is the hydrodynamic radius, L is the rod length, d is the diameter of the rod, r is the disk radius, and t is the disk thickness. A nonlinear least-squares fitting program based on the Marquardt algorithm (Marquardt, 1963) was used to determine the parameters that provided the best theoretical fit of the mixed-disk and capped-rod models to the data. The best-fit parameters for the mixed disk model are $2p/\sigma = 23.9$ Å and $\gamma = 1.55$. Those for the capped rod model are $\alpha/\beta = 1.40$, $a/b = 0$, and $2b/\beta = 81.6$ Å. The theoretical plots of the rod lengths and disk radii were converted back to hydrodynamic radii by using eq 4 and 5, and the results are plotted in Figure 3 (dotted line, mixed-disk model; dashed line, capped-rod model). The standard error [(sum of the squares of the differences)/(number of observations minus number of parameters) minus 1] for the hydrodynamic radii plots are 60.5 for the mixed-disk model and 50.1 for the capped-rod model. The capped-rod model fits the data slightly better than the mixed-disk model, although the error in these measurements is too large to allow discrimination between the two.

The parameters obtained from the best-fit procedure should correspond to reasonable molecular dimensions of phospholipid and bile salt given the constraints of each model. Mazer et al. (1980) predicted the expected values for the parameters $2p/\sigma$ and γ as described below. Assuming σ, the number of lecithin molecules per unit area of the mixed bilayer is equal to $2/A_L$, where A_L is the measured surface area in a bile salt saturated bilayer (60–70 Å^2; Small & Bourgès, 1966), and p, the number of bile salts per unit length of the disk's perimeter, is equal to $2/W$, where W is the width of the bile salt on the disk's perimeter (7–9 Å; estimated from molecular models, Small, 1971). Thus, $2p/\sigma$ is expected to be in the range of 13–20 Å which is close to the best-fit value of 23.9 Å. The best-fit value of γ (1.55) is also consistent with the maximum amount of bile salt that can be obtained in the bile salt–lecithin lamellar phase (Small & Bourgès, 1966).

A similar analysis demonstrates that the three parameters obtained for the capped-rod model from the least-squares analysis of the data in Figure 3 are consistent with estimated molecular dimensions of lecithin and bile salt. By use of the molecular surface area (70 Å^2; Small & Bourgès, 1966) derived from X-ray crystallography of lecithin–bile salt mixtures and half the length of a lecithin bilayer determined from X-ray crystallography of lecithin bilayers (27 Å; Franks & Lieb, 1981), the molecular volume of a lecithin molecule is calculated to be 1890 Å^3. According to space-filling models, bile salts are roughly cylinders with 3.5-Å radii and a length of 20 Å (Small, 1971), which gives an estimated molecular volume of 769 Å^3. A rod with a 27-Å radius and a length of 100 Å has a volume of 228 910 Å^3. When the estimated molecular volumes and the lecithin to bile salt ratio predicted by the model ($a/b = 1.40$) are used, the numbers of lecithin and bile salt molecules in this rod are calculated to be 94 and 67, respectively. Assuming that the lecithin molecules are oriented radially around the long axis of the rod with their head group facing outward, the molecular surface area of the phospholipids in the rod would be expected to be close to that in a bilayer (70 Å^2). On the basis of this assumption, the bile salts must contribute 10 380 Å^2 to the total surface area (16 960 Å^2) of the 100-Å-long rod which predicts a molecular

surface area for the deoxycholate molecules of 155 Å^2. This number is very close to the 140 Å^2 predicted from molecular models assuming that the deoxycholate molecules lie flat along the surface of the rod with their polar sides facing outward. A monomeric or dimeric arrangement of bile salts intercalated between the phospholipids would not provide a sufficient surface to volume ratio to satisfy the rod configuration.

The number of deoxycholate molecules contained in each cap can be calculated from the fit parameter $2b/\beta = 81.6$ Å, since we have already calculated the number of bile salts in a 100-Å rod of 27-Å radius ($\beta = 67/100$ Å). Thus, $b = 27$ deoxycholate molecules per cap, and since $a/b = 0$, the caps contain no phospholipids.

The estimates of the number of molecules per length and per cap have been combined with the measured size of the micelle radius to draw a scaled diagram of the capped-rod model for deoxycholate and POPC micelles. This diagram uses reasonable estimates of the molecular dimensions of phosphatidylcholine and bile salt and illustrates how they can combine to form a rod-shaped micelle. The bile salt molecules at the surface of the micelle separate the phospholipid head groups, forcing them into a radial micellar orientiation as opposed to a planar bilayer.

The structural arrangement presented in Figure 4 is not meant to be taken literally. As shown, the best fit of the phospholipid–deoxycholate data (Figure 3) indicated that only deoxycholate was contained in the caps. Perhaps fortuitously the predicted number of deoxycholate molecules in the cap provides just enough surface area to cover the exposed ends of the rod as a single layer. However, the data in Figure 3 are not sufficiently accurate to rule out other possible cap conformations, such as a hemispherical or conical arrangement of lecithin and bile salts. The model itself makes no assumptions about the shape of the caps but only requires that the phospholipid to bile salt ratio be less in the cap than in the rod portion.

Since both the mixed-disk and capped-rod models provide reasonable fits to the data in Figure 3 with parameters that are consistent with the molecular dimensions of lecithin and bile salt, size data alone cannot resolve the structure of these micelles. However, the size data demonstrated that the capped-rod model provides a reasonable alternative to the mixed-disk model, with a rational explanation of how phospholipids and bile salts can aggregate into rod-shaped micelles that is consistent with phospholipid and bile salt molecular dimensions and which explains micellar growth as a function of the phospholipid to bile salt ratio in the micelle. This model should be useful in directing future studies to determine conclusively the structure of the lecithin–bile salt mixed micelle.

Acknowledgments

We thank Adrienne McLean for the expert artwork and editorial assistance and Bill Goolsby for providing the nonlinear least-squares fitting program.

References

Ackers, G. K. (1967) *J. Biol. Chem. 242*, 3237–3238.
Ames, B. N., & Dubin, D. T. (1960) *J. Biol. Chem. 235*, 769–775.
Franks, N. P., & Lieb, W. R. (1981) in *Liposomes: From Physical Structure to Therapeutic Applications* (Knight, C. G., Ed.) Chapter 8, Elsevier/North-Holland, Amsterdam.
Himmel, M. E., & Squire, P. G. (1981) *J. Chromatogr. 210*, 443–452.
Hjelm, R. P., Jr., Thiyagarajan, P., & Alkan, H. (1988) *J. Appl. Crystallogr. 21*, 858–863.
Hjelm, R. P., Jr., Thiyagarajan, P., & Alkan, H. (1990) *Mol. Cryst. Liq. Cryst. 180A*, 155–164.
Kumosinski, T. F., & Pessen, H. (1985) *Methods Enzymol. 117*, 154–182.
Lindblom, G., Eriksson, P.-O., & Arvidson, G. (1984) *Hepatology 4*, 1295–1335.
Marquardt, D. W. (1963) *J. Soc. Ind. Appl. Math. 11*, 431–441.
Mazer, N. A., Benedek, G. B., & Carey, M. C. (1980) *Biochemistry 19*, 601–615.
Menger, F. M., Lee, J.-J., Aikens, P., & Davis, S. (1989) *J. Colloid Interface Sci. 129*, 185–191.
Müller, K. (1981) *Biochemistry 20*, 404–414.
Müller, K. (1984) *Hepatology 4*, 134s–137s.
Nichols, J. W. (1988) *Biochemistry 27*, 3925–3931.
Nozaki, Y., Schecter, N. M., Reynolds, J. A., & Tanford, C. (1976) *Biochemistry 15*, 3884–3890.
Ollivon, M., Walter, A., & Blumenthal, R. (1986) *Anal. Biochem. 152*, 262–274.
Roda, A., Hofmann, A. F., & Mysels, K. J. (1983) *J. Biol. Chem. 258*, 6362–6370.
Schurtenberger, P., & Lindman, B. (1985) *Biochemistry 24*, 7161–7165.
Schurtenberger, P., Mazer, N., & Känzig, W. (1985) *J. Phys. Chem. 89*, 1042–1049.
Shankland, W. (1970) *Chem. Phys. Lipids 4*, 109–130.
Small, D. M. (1971) in *The Bile Acids: Chemistry, Physiology and Metabolism* (Nair, P. P., & Kritchevsky, D., Eds.) pp 249–355, Plenum Press, New York.
Small, D. M., & Bourgês, M. (1966) *Mol. Cryst. 1*, 541–561.
Smith, R., & Tanford, C. (1972) *J. Mol. Biol. 67*, 75–83.
Snedecor, G. W., & Cochran, W. G. (1967) *Statistical Methods*, 6th ed., pp 155–157, Iowa State University Press, Ames, IA.
Tables of the Error Function and Its Derivitive (1954) *NBS Applied Mathematics Series 41*, United States Government Printing Office, Washington, D.C.
Vinson, P. K., Talmon, Y., & Walter, A. (1989) *Biophys. J. 56*, 669–681.
Walter, A., Vinson, P. K., & Talmon, Y. (1990) *Biophys. J. 57*, 476a.